Homogenization of Functionals with Linear Growth in the Context of $$mathcal A$$ A -quasiconvexity

Energy 302 (2024) 131871

Contents lists available at ScienceDirect

Energy

journal homepage: www.elsevier.com/locate/energy

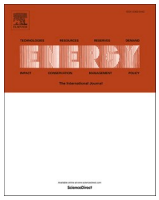

Exploring opportunities for temperature reduction in existing district heating infrastructures

Martina Capone *, Elisa Guelpa, Vittorio Verda

Energy Department, Politecnico di Torino, Corso Duca Degli Abruzzi 24, 10129, Torino, Italy

ARTICLE INFO

Handling Editor: Dr. Henrik Lund

Keywords:
District heating networks
Low temperature systems
Pumping optimization
Supply temperature reduction
Thermal network

ABSTRACT

The integration of renewable energy sources into existing district heating systems is imperative for the decarbonization of the global energy system. This transition is particularly challenging in existing systems that were originally supplied by fossil fuel plants and designed to operate with high supply temperatures. Reducing supply temperatures to facilitate the integration of low exergy heat may not be suitable for the existing infrastructure, due to both the heating devices or the thermal substations that may not support significant reductions or to the distribution infrastructure that can be unable to handle the required mass flow rate increases. To address these challenges, this paper focuses on the distribution infrastructure by introducing a physical-based approach to explore the current potential for supply temperature reduction of existing district heating infrastructures, taking into account the hydraulics of the system. Indeed, being able to identify the possible hydraulic bottlenecks arising in the network is essential to enable the transition of the networks and requires an accurate modelling of the fluid dynamic of the system. The methodology is fast and versatile, making it suitable for applications from small-scale to large-scale systems. An application to a real large-scale network is presented, proving the wide applicability of the methodology. Promising results in terms of temperature reduction are shown to be possible: the analyzed infrastructure is currently capable of shifting its operation from 120 °C to about 102 °C without considering invasive structural interventions on the network, and further reductions up to 90 °C are conceivable by assuming some adjustments to the system configuration.

1. Introduction

Tackling climate change is one of the biggest tasks of today's society. Challenging objectives have been set by the European Union, aiming to become a climate-neutral economy by 2050, with an interim target of reducing greenhouse gas emissions by 55 % by 2030 compared to 1990 levels [1]. Considering that heating represents the world's largest energy end-use and is currently heavily reliant on fossil fuels [2], decarbonizing the heating sector becomes imperative for attaining these targets. To achieve this goal, District Heating (DH) is nowadays widely acknowledged as one of the most relevant solutions for the decarbonization of heat supply in cities, being regarded as a driving technology for reducing environmental impact while maintaining competitive costs [3]. Indeed, while early networks were supplied by centralized fossil-fuel heating plants, next-generation systems allow for ever-increasing penetration of waste heat and renewable energy sources, and increasingly incorporate digital technologies and smart grids for greater efficiency and sustainability [4–6].

For a cost-effective decarbonization of the European energy system, it is essential to bolster the diffusion of efficient DH not only by building new-generation networks but also by prioritizing a major effort in the refurbishment of existing infrastructures [7]. This assumes a special relevance given the substantial presence of outdated DH systems in place today in Western Europe, primarily linked to the early adoption of DH technologies in some regions [8].

An urgent requirement for this renovation is the adaptation of existing networks to operate at lower temperatures. Older networks were initially designed to function with high temperatures provided by fossil fuel plants, while the transition to renewables involves operation at lower temperatures [9,10], posing significant challenges as the existing infrastructure, originally designed for different conditions, may not seamlessly accommodate the required temperature settings [11,12].

1.1. Potential and limitations for lowering temperature levels

The benefits of reducing operating temperatures in DH infrastructure

* Corresponding author.
E-mail address: martina.capone@polito.it (M. Capone).

https://doi.org/10.1016/j.energy.2024.131871
Received 19 December 2023; Received in revised form 23 May 2024; Accepted 29 May 2024
Available online 31 May 2024

have been thoroughly documented in the literature [13,14]. Positive impacts can be achieved at the supply, distribution, and consumption levels:

- The benefits at the supply level are certainly the driving force behind the transition to low-temperature networks, as temperature reduction is a prerequisite for the integration of heat from renewable energy sources. With lower temperatures, it would be possible to integrate heat from solar heating plants, geothermal heat, and waste heat from industrial processes, data centers or supermarkets. The possibility of connecting prosumers would also become of central relevance [15]. Finally, the use of heat pumps would be encouraged, further enhancing the penetration of renewables and making it possible a cross-sector integration of heating and electricity systems [16,17].
- Substantial benefits can be identified at the distribution level as well. In this case, a key advantage is linked to the notable reduction in heat losses, which can be significantly reduced even in existing networks [18]. Other minor advantages include the feasibility of using plastic pipes in specific areas, a decrease in the risks of water boiling and pipe leakages attributed to thermal stress, and a lower risk of skin burns for workers during pipe maintenance [19,20].
- Finally, reducing the operating temperature on the consumer side leads to a performance improvement relying on a better quality match between demand and supply: through an exergy analysis of the entire system, Li and Svendsen [21] showed that domestic hot water (DHW) and space heating (SH) preparation represents the largest exergy loss in the system and that shifting to lower temperatures brings to relevant improvements in the exergy efficiency and, as a consequence, in the system performance itself. Temperature reductions on the consumer side can be implemented in both primary and secondary circuits, depending on the specific characteristics of substations and heating equipment. On the secondary side, they can be achieved by using radiant heating devices with large heating surface (e.g. floor, ceiling, or wall heating), which can deliver the required heating power to the building using supply temperatures only few degrees above the thermal comfort temperature in the case of new buildings [22]. In general, customers of DH services could benefit from temperature reduction in the system due to the potential price reductions associated with efficiency improvements [23], besides having the possibility of being connected through bidirectional substations to sell heat to the network in case of surplus heat production [24].

Existing studies on this topic are mainly focused on the realization of low temperature (LTDH) and ultra-low temperature district heating (ULTDH) [25,26]. The feasibility and market-readiness of these technologies are demonstrated by different case studies: Schmidt et al. [27] analyzed 15 cases of successful implementation of LTDH in Europe under different boundary conditions. A feasibility study of ULTDH with solar thermal systems was carried out by Lumbreras and Garay [28] considering three different climates (Spain, France, and Denmark). Different opportunities for low-temperature DH implementation were analyzed by Werner [29], who proposed an inventory of fourteen possible network configurations suitable for LTDH.

Additional challenges arise when trying to implement LTDH in already existing networks, designed and currently running with higher supply temperatures. These networks, originally configured for different conditions, may not be adequately equipped to operate with significantly lower temperatures. In this case, the implementation of low temperature sub-networks has been proposed by several studied [30–32] as a potential solution to enhance the sustainability of the system and overcome the possible limitations of transforming the whole high temperature system into LTDH. In order to achieve the full transformation of the existing DH infrastructures, a research project was financed by IEA-DHC within Annex XIII with the purpose of identifying and addressing the main limitations to the temperature reduction in small-to-large scale systems [14]. These limitations can occur at different levels:

- Starting from the building-level, the heating devices that are installed in the buildings can be unsuitable for operation at much lower temperatures than those for which they are designed (this value is typically around 70–80 °C for radiators and 40–45 °C for floor heating). However, by analyzing the literature, it turns out that many heating devices that are currently present in the buildings are actually capable of operating at low supply temperatures [33,34]. As an example, the investigation conducted by Hesaraki et al. [34] proved that thermal comfort can be guaranteed by providing water at around 45 °C in conventional radiators and 30 °C for floor heating. This means that meaningful temperature reductions can be achieved in the secondary circuit of DH systems even when conventional heating devices are installed.
- Secondly, there could be limitations at substation level, arising when the area of the heat exchanger is insufficient to provide the required thermal demand to the building when the supply temperature is reduced. Indeed, with a given heat exchanger, the reduction in the supply temperature at the primary circuit causes a reduction in the temperature drop (which is due to the fact that the return temperature presents a lower reduction than the supply temperature); thus, to provide the same thermal power to the buildings, an increase in the mass flow rate is needed; in some circumstances, a too low supply temperature could make the operation unfeasible for the substation installed, due to the excessive mass flow rate that would be required. This limitation was addressed in detail in Ref. [35], where a methodology was proposed to assess the current potential for supply temperature reduction allowed by substations that are already installed, which was quantified to be about 30 °C (from 120 °C to about 90 °C) in the substations analyzed; specifically, the authors considered acting only on the primary circuit, while leaving the temperature in the building heating circuit unchanged; even greater reductions could be obtained if interventions would also be allowed on the secondary circuit.
- Finally, the network infrastructure can be unsuitable to support the mass-flow rate increase that is required by the substations to operate with lower temperatures and that can cause water congestion in some areas of the network [36]. The identification of the current potential of supply temperature reduction that is possible in the networks is discussed in this study.

1.2. Research gap

In this context, the research gap identified and addressed is marked by the absence of a physical-based approach to evaluate the potentialities of supply temperature reduction in existing DH networks, considering both the transportation infrastructure and the substation side. The evaluation of these potentialities is challenging and requires an accurate knowledge of the physics of the system. This becomes particularly complex in large-scale networks, especially those with looped topologies and many degrees of freedom to determine their operation. To address this research need, a methodology is developed to identify the potential for temperature reduction that can be currently implemented in a DH network already installed and designed to operate with different conditions, with a focus on the hydraulics of the system. The methodology includes an optimization approach that allows maximizing the mass flow circulating in the network while keeping as lower as possible the pumping power increase. The development of the methodology takes into account the necessity for a fast and versatile approach, making it applicable to diverse case studies from small to large scale size and able to describe the real-world complexities of DH networks.

The methodology discussed in this paper allows evaluating the current potential for supply temperature reduction by acting on the existing

elements of the system: the pressure rise of the pumping stations can be differently managed to properly distribute mass flow rates among the different looping branches in order to enhance the potential reduction for supply temperature, without the need of replacing specific elements of the infrastructure.

An application to a relevant case study is proposed in this work, involving a large-scale DH network originally designed to be supplied by superheated hot water. Additional strategies are also discussed to further improve the prospective supply temperature reduction to be implemented in the network.

2. Methodology

The reduction of supply temperatures in existing DH infrastructure leads to a significant rise in the mass-flow rate necessary for substations to fulfill the same thermal demand; this is associated to the fact that when the supply temperature decreases, the return temperature experiences a lower reduction than the supply, as discussed in Ref. [35]. Even if the substations can accommodate the higher mass flow, it is imperative for the distribution infrastructure itself to support this increase without creating fluid-dynamic bottlenecks or water congestion in some network areas: these occur when some of the pipes installed in the network are too small to sustain the increase in the mass flow rate, jeopardizing the possibility of further temperature reduction or even possible expansion of the network. For this reason, it is essential to have a tool to quantify the potential temperature reduction, which is associated with the mass flow rate increase that is possible to achieve with the installed piping. In this section, a methodology is developed to quantify the potential for supply temperature reduction in existing infrastructures taking into account not only the temperature requirements of the substations but also the hydraulics of the network, which is the main focus of the study. The network infrastructure is considered as it is, with given location of the installed thermal plants, configuration and size of the network pipelines, pumping stations, substations and building's operation. Structural interventions in the network are not considered in this work, which only aims to estimate the existing potential, acting exclusively on the pressure rise of the installed pumps, without accounting for possible modifications to the infrastructure.

2.1. Main objectives

The objective of the analysis is to identify the minimum temperature achievable by DH networks, taking into account the hydraulics of the system. This goal is pursued through a two-step methodology:

- **Step 1**: Maximizing mass flow rate and optimizing pumping configuration (Section 2.3)

The initial step is focused on identifying the maximum sustainable increase in mass-flow rate by the network, taking into account pipeline oversizing and potential adjustments to pumping stations. This is accomplished through the solution of an optimization problem designed to maximize the circulating mass-flow rate by acting on the pumping system (Step 1a). This step of the methodology also includes the identification of the best operation setup associated with the new configuration; this is achieved through the solution of a further optimization problem that allows optimally managing the pumps such that the pumping power required by the new operating conditions is minimized, in order to limit the increase in the costs associated with the increase of the mass flow rate (Step 1b). This is necessary because there may be different combinations of pressure increases that produce the same results in terms of maximum mass flow: Step 1a only ensures the maximization of mass flow, but not necessarily the corresponding minimization of total pumping cost, which is what Step 1b is designed to do. To perform the two optimization problems, a fluid-dynamic model of the network is needed to guarantee the satisfaction of all the physical constraints while managing the free variables of the problem: the model is nested in both the optimization steps and is explained in detail in Section 2.2.

- **Step 2**: Determining the corresponding supply temperature reduction (Section 2.4)

The second step involves determining the minimum feasible temperature level in the considered network, corresponding to the identified maximum increase in mass-flow rate. This requires cross-referencing the results of the optimization at network level with the mass-flow rate increases determined by the substation analysis.

The methodology is suitable for application to DH networks of different sizes, including large scale networks with complex topologies.

2.2. Fluid-dynamic model of the district heating network

In order to verify the satisfaction of the DH network constraints, a fluid-dynamic simulation is needed to test the changed operating conditions, evaluating the pressures and velocity distributions within the network.

The formulation of the fluid-dynamic model is based on the thermo-fluid dynamic model presented in previous works [37,38]. The fluid-dynamic problem is analyzed in steady-state conditions since the pressure perturbations are quickly transferred to the network. A one-dimensional formulation is adopted, where the topology of the network and the interconnections among the different pipes are taken into account through the graph theory [39]: each pipe is represented as a branch connecting the inlet node to the outlet node, while the nodes represent the junctions among the different pipes/branches. The incidence matrix **A** describes the topology of the network: it has a number of rows equal to the number of nodes (NN) and a number of column equal to the number of branches (NB); the generic element A_{ij} is equal to 1 if the i-th node is the inlet node of the j-th branch, -1 if the i-th node is the outlet node of the j-th branch, and 0 if the i-th node and the j-th branch are not connected.

The fluid-dynamic model is applied to the whole network by taking advantage of the finite volume method. The mass conservation equation is applied to control volumes including each node and half of the pipes entering or existing the specific node, while the momentum conservation equation is applied to control volumes including each pipe and the corresponding inlet and outlet nodes. The problem can be expressed by the following systems of equations, written in matrix form:

$$\mathbf{AG} + \mathbf{G}_{\text{ext}} = \mathbf{0} \tag{1}$$

$$\mathbf{A}^{\mathbf{T}}\mathbf{P} = \mathbf{R}(\mathbf{G})\mathbf{G} - \mathbf{t} \tag{2}$$

Equation (1) is the system of linear equations representing the mass-conservation equations, while Equation (2) is nonlinear and represents the momentum conservation equations. The unknowns of the problem are represented by the column vectors **G** (mass-flow rates in the branches, length NB) and **P** (pressures in the nodes, length NN). The model is applied both to the supply network and to the return, by defining also proper boundary conditions for each case; thus, the total number of unknowns is 2(NN + NB). The boundary conditions of the problem are represented by the vector $\mathbf{G}_{\text{ext}}$ (length NN) and by a pressure boundary condition that must be applied to one node of the network (usually one plant); specifically, $\mathbf{G}_{\text{ext}}$ contains the mass-flow rates injected or extracted from each control volume: in the supply network, there are injections in the nodes corresponding to production plants and extractions in the nodes corresponding to the buildings; vice versa in the return network, injections are from the buildings and extractions from the plants; as for the pressure boundary condition, it must be imposed by adding a further equation $\mathbf{P}(n_{BC}) = p_{BC}$ since the system of expressions contained in Eq. (2) accounts only for the pressure differences in the various branches. Beside the incidence matrix, the unknowns and the

boundary conditions, the other terms contained in the expressions are the matrix **R** and the column vector **t** :

- The matrix **R** is the hydraulic resistance matrix (size NB × NB) and contains in the diagonal the terms associated with the pressure losses in the different branches, as expressed by Equation (3): G_j is the mass-flow rate in the j-th branch; ρ is the density of the fluid, assumed as constant; S_j, L_j, D_j are respectively the section, length, and diameter of the j-th branch; f is the friction factor, and β the localized pressure drop coefficient.

$$R_{j,j} = \frac{1}{2}\frac{|G_j|}{\rho S_j^2}\left(f\frac{L_j}{D_j} + \sum \beta_j\right) \tag{3}$$

- Finally, the vector **t** takes into account for the pressure rise due to the pumps. The generic element t_j is different than zero when a circulation pump is present in the j-th branch. In general, circulation pumps of a DH system can be located at different locations of the network: besides pumps at the thermal plant, booster pumps are generally located within the network. For illustrative purposes, a sample network is reported in Fig. 1. Boosting pumps allow avoiding high pressure within the network and high pressure-gaps at plant pumping stations: in Fig. 2, an example of the pressure evolution of water supplied to a building with and without the presence of two booster pumps is reported; the maximum pressure reached in case no booster pumping stations are used is labeled as point B. It is straightforward to understand that a proper management of the pumping power of each pump can lead to significant pressure reductions and, consequently, to the possibility of circulating more mass-flow rate within the transportation infrastructure. In case of looped topologies, as for example the one reported in Fig. 1, the regulation of the pressure rise of the different pumps also allows to differently distribute mass flow rates in the various looping branches, contributing in this way to the determination of the total pressure losses in the network.

Due to the strict coupling between mass and momentum conservation equations, it is usually required to adopt an iterative algorithm to solve the problem. The SIMPLE algorithm (Semi-Implicit Method for Pressure-Linked Equations) introduced by Patankar and Spalding [40] can be efficiently applied to this purpose, as previously done in different DH applications [41]. An alternative strategy to solve the problem is to reformulate it into a constrained feasibility problem; this can be achieved by casting the unknowns **G** and **P** as fictitious optimization variables and the model equations (Eq. (1) and Eq. (2)). as optimization constraints. With this reformulation, the problem can be solved using an optimization algorithm that allows finding the unique combination of **G** and **P** that satisfies all the constraints. This reformulation is applicable both to simulation and to cases where the original problem to be solved is itself an optimization; in this case, additional variables and constraints can be incorporated into the original optimization problem. The technique adopted in this work, elaborated further in Section 2.3, is an example of this reformulation approach.

2.3. Step 1: maximization of mass flow rate and minimization of pumping power

The first step of the analysis consists in the identification of:

a) the maximum mass flow rate allowed to circulate in the network (*Step 1a*);
b) the minimum pumping power associated with the new configuration with increased mass flow rate (*Step 1b*);

These two objectives are pursued by developing and implementing two subsequent optimization problems, which are described in detail in this section.

2.3.1. Step 1a: maximization of mass flow rate

The optimization approach developed to address the first part of the problem is summarized in Fig. 3. The purpose of the figure is to explain how the problem of supply temperature minimization is converted into a maximization of mass flow rate and how the problem can be then implemented. The following considerations can be done:

- Problem definition. The goal of this work is to minimize the supply temperature (objective function) of a certain existing network, considering the installed infrastructure and assuming that actions can be taken exclusively to regulate the pressure rise of the different pumping stations (optimization variables). Once the reduction potential at the building and substation level has been identified (this can be done by adopting the methodology proposed in Ref. [35] and briefly explained in Step 2 of this analysis), it is crucial to assess the potential of the network infrastructure. This is determined by the maximum mass-flow rate increase required by the substations that can be supported by the network. Naturally, when reducing the supply temperature, the constraints of the network must be respected, paying attention a) to not exceed the maximum pressure allowed in the pipes which is determined by the manufacturer, b) not to go below the minimum pressure required to prevent evaporation risks, and c) to observe the velocity limitations. These are the optimization constraints that must satisfied for both the supply and return networks.
- Equivalent optimization problem. Since the supply temperature reduction is strictly related to the mass-flow rate increase, an equivalent optimization problem is defined. The objective is to maximize the mass-flow rate increase that can be applied to the different buildings connected to the network. To this purpose, a new variable β is defined, representing the multiplication factor for the mass-flow rates boundary conditions: the extracted mass flow rate vector is thus formulated as $\mathbf{G}_{ext} = \beta \mathbf{G}^{0}_{ext}$, where $\mathbf{G}^{0}_{ext}$ contains the mass flow boundary conditions for the reference scenario (no temperature reduction). In this work, it is assumed that the increase in mass-flow rate is uniformly distributed throughout the network. Although it is true that in some areas of the network there could be a higher increase with respect to the most critical zones, this assumption allows to have a uniform temperature reduction and to define a unique supply temperature value for the whole network; areas with a higher potential of supply temperature reduction can then be identified through a further analysis of the results obtained.

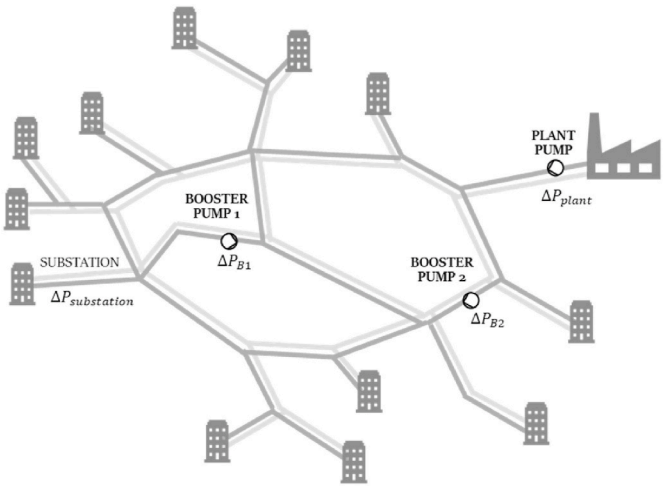

Fig. 1. Schematic of a sample network with a loop topology.

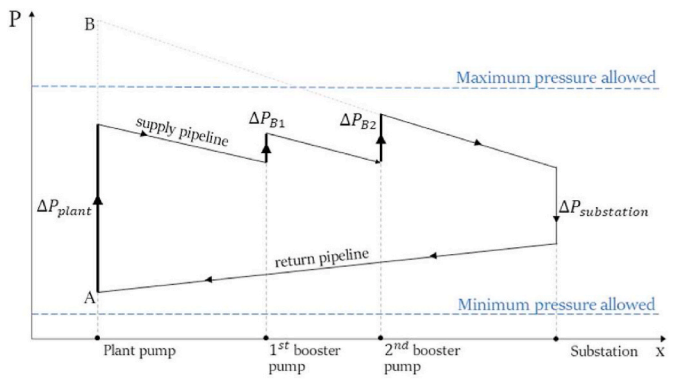

Fig. 2. Comparison of the pressure distribution with and without booster pumping stations for a sample linear network with one thermal plant and one thermal customer.

referred to Section 2.2.

- Reformulation of the equivalent optimization problem. Finally, the optimization problem is reformulated to reduce nonlinearities. The first step of the reformulation consists in the transformation of the simulation model function into constraints of the optimization problem. This is achieved, as explained in Section 2.2, by considering the vectors **G** and **P** as fictitious optimization variables. With these auxiliary functions, the simulation model can be expressed by adding equality constraints to the optimization problem that can be rewritten as in Equation (5) .[1]

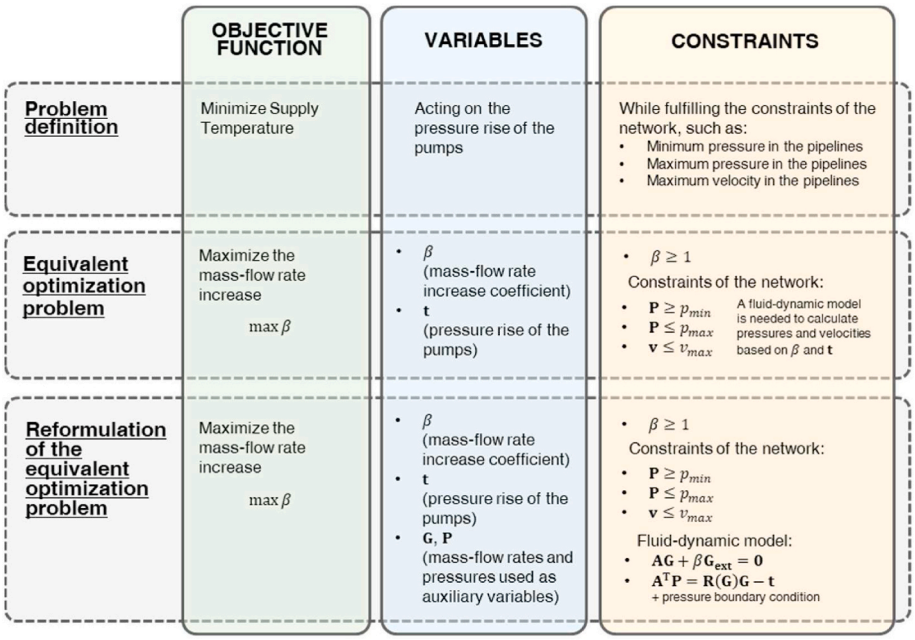

Fig. 3. Outline of the different levels of the reformulation approach adopted for step 1a.

The mass-flow rate increase coefficient β is one of the independent variables of the optimization problem, as well as being the objective function to be maximized. The other independent variables that can be manipulated to achieve the above objective are the pressure rises of the different pumps that are installed along the network, contained in the vector **t**. The optimization constraints to be satisfied are the provision of a sufficient mass-flow rate to the buildings (meaning that the mass-flow rate cannot be lower than the current value, i.e. $\beta \geq 1$) and the aforementioned pressure and velocity constraints on the network. Thus, the evaluation of the network constraints requires the solution of the nonlinear fluid-dynamic model of the DH network. Overall, the optimization problem can be written as in Equation (4):

$$\max_{\beta,\mathbf{t}} \beta \; s.t. \begin{cases} \beta \geq 1 \\ \mathbf{P}(\mathrm{f}(\beta,\mathbf{t})) \geq p_{min} \\ \mathbf{P}(\mathrm{f}(\beta,\mathbf{t})) \leq p_{max} \\ \mathbf{v}(\mathrm{f}(\beta,\mathbf{t})) \leq v_{max} \end{cases} \tag{4}$$

where $\mathrm{f}(\beta,\mathbf{t})$ is a function for the simulation of the fluid dynamic model of the network, which varies according to the given inputs β and **t**. For an explanation of the simulation model, the reader is

$$\max_{\beta,\mathbf{t},\mathbf{G},\mathbf{P}} \beta \; s.t. \begin{cases} \beta \geq 1 \\ \mathbf{P} \geq p_{min} \\ \mathbf{P} \leq p_{max} \\ \mathbf{G} \leq \rho v_{max} \mathbf{S} \\ \mathrm{AG} + \beta \mathbf{G}^0_{\mathrm{ext}} = \mathbf{0} \\ \mathbf{A}^{\mathbf{T}}\mathbf{P} = \mathbf{R}(\mathbf{G})\mathbf{G} - \mathbf{t} \\ \mathbf{P}(n_{BC}) = p_{BC} \end{cases} \tag{5}$$

[1] For the sake of simplicity, all the constraints are written only once, but it is important to underline that the optimization variables **G** and **P** should be considered for both the supply and the return networks, as well as the optimization constraints containing **G** and **P** should be written for both distribution lines. Moreover, the lower and upper boundaries for the pressure are actually imposed on the static pressures, which are evaluated taking into account also the contributions given by the altitude, included in the vector **z**; these contributions are omitted in the text for better readability. The complete formulation of the problem is reported in the Appendix.

Being the matrix $\mathbf{R}$ dependent on the mass-flow rate $\mathbf{G}$, the optimization problem is nonlinear. A further nonlinearity is given by the fact that the dependency between $\mathbf{R}$ and $\mathbf{G}$ also contains an absolute value, as reported in Equation (3). In general, the matrix $\mathbf{R}$ can be written as the Hadamard product of a matrix $\mathbf{r}$ and the absolute value of the mass-flow rate vector $\mathbf{G}$: $\mathbf{R} = \mathbf{r} \odot |\mathbf{G}|$, making the problem read as in Equation (6) [1]:

$$\max_{\beta,\mathbf{t},\mathbf{G},\mathbf{P}} \beta \; s.t. \begin{cases} \beta \geq 1 \\ \mathbf{P} \geq p_{min} \\ \mathbf{P} \leq p_{max} \\ \mathbf{G} \leq \rho v_{max} \mathbf{S} \\ \mathrm{AG} + \beta \mathbf{G}^0_{\mathrm{ext}} = \mathbf{0} \\ \mathbf{A}^{\mathrm{T}} \mathbf{P} = (\mathbf{r} \odot |\mathbf{G}|)\mathbf{G} - \mathbf{t} \\ \mathbf{P}(n_{BC}) = p_{BC} \end{cases} \tag{6}$$

The nonlinearities can be reduced by doing a further reformulation of the problem that is meant to linearize the absolute value. This can be done by introducing auxiliary Big-M constraints and auxiliary continuous and binary variables. The auxiliary continuous variables are summarized in the column vector $\mathbf{G}_{\mathrm{aux}}$, which represents the absolute value of $\mathbf{G}$; the auxiliary binary variables are contained in the column vector $\mathbf{B}$, whose generic element B_j is equal to 1 when the mass-flow rate is negative and 0 otherwise. The auxiliary constraints that need to be introduced are those reported in Equation (7) [1]:

$$\begin{cases} \mathbf{G} + M\mathbf{B} \geq \mathbf{G}_{\mathrm{aux}} \\ -\mathbf{G} + M(\mathbf{1} - \mathbf{B}) \geq \mathbf{G}_{\mathrm{aux}} \\ \mathbf{G}_{\mathrm{aux}} \geq \mathbf{G} \\ \mathbf{G}_{\mathrm{aux}} \geq -\mathbf{G} \end{cases} \tag{7}$$

Using these constraints, when $B_j = 1$, the first constraint is always fulfilled (since it basically translates into $G_{aux,j} \leq \infty$). The second constraint, reading $G_{aux,j} \leq -G_j$, together with the fourth constraint imposing $G_{aux,j} \geq -G_j$, enforces $G_{aux,j} = -G_j$. The third constraint $G_{aux,j} \geq G_j$ defines that this situation happens when G_j is negative, as it constrains the auxiliary variable to be greater than the corresponding variable. Vice versa, when $B_j = 0$, the first, third and fourth constraints are active, while the second constraint is always satisfied. The first imposes $G_{aux,j} \leq G_j$, and combined with the third saying that $G_{aux,j} \geq G_j$, enforces $G_{aux,j} = G_j$. Finally, the fourth constraint $G_{aux,j} \geq -G_j$ defines that this situation happens when G_j is positive. Through these modifications, the full optimization problem can be rewritten as in Equation (8) ,[1] where M represents a sufficiently large number:

$$\max_{\beta,\mathbf{t},\mathbf{G},\mathbf{P},\mathbf{G}_{\mathrm{aux}},\mathbf{B}} \beta \; s.t. \begin{cases} \beta \geq 1 \\ \mathbf{P} \geq p_{min} \\ \mathbf{P} \leq p_{max} \\ \mathbf{G} \leq \rho v_{max} \mathbf{S} \\ \mathrm{AG} + \beta \mathbf{G}^0_{\mathrm{ext}} = \mathbf{0} \\ \mathbf{A}^{\mathrm{T}} \mathbf{P} = (\mathbf{r} \odot \mathbf{G}_{\mathrm{aux}})\mathbf{G} - \mathbf{t} \\ \mathbf{P}(n_{BC}) = p_{BC} \\ \mathbf{G} + M\mathbf{B} \geq \mathbf{G}_{\mathrm{aux}} \\ -\mathbf{G} + M(\mathbf{1} - \mathbf{B}) \geq \mathbf{G}_{\mathrm{aux}} \\ \mathbf{G}_{\mathrm{aux}} \geq \mathbf{G} \\ \mathbf{G}_{\mathrm{aux}} \geq -\mathbf{G} \end{cases} \tag{8}$$

By employing this reformulation approach, the original MINLP optimization problem is converted into a MIQCP (Mixed Integer Quadratically Constrained Program) and can be efficiently solved through using an appropriate solver. The reformulation allows for a faster solution than what a MINLP would require due to the inherent complexity and nonlinearities in the original problem. In this study, the MIQCP optimization problem is implemented in the Julia language [42] and solved using the Gurobi Optimizer [43] as solver. The following results can be obtained from the optimization:

- the maximum increase of mass-flow rate that can be operated to the analyzed network;
- an optimal setting of the pressure rise of the different pumping stations that allow to maximize the mass-flow rate;
- the corresponding distribution of pressures and mass-flow rates in the network.

2.3.2. Step 1b: minimization of the pumping power

The optimization methodology discussed in Section 2.3.1 allows determining the maximum increase in the mass flow rate that can be sustained by the network infrastructure and the corresponding minimum supply temperature achievable. This improvement in the operation of the network is obtained by acting on the pressure rise of the different pumps located in the network. However, it is essential mentioning that there can be different combinations of pressure rise of the pumps bringing to the same mass flow increase/supply temperature decrease. While the different combinations may not be equally convenient, the optimizer presented in the previous sections does not make a distinction between them, thus producing a result that is optimal in terms of maximum mass flow (and, as a consequence, minimum supply temperature) but not necessarily optimized in terms of total pumping cost.

For this reason, a further optimization step is proposed with the aim of minimizing the total pumping power in the new configuration. The optimization problem can be expressed by the formulation proposed in Equation (9) .[1] The structure is similar to the one proposed for the maximization of the mass flow rate coefficient, including the network constraints and the fluid-dynamic model. The main differences are the following:

- the coefficient β is no more an optimization variable, while it is a constant established by the result of the previous optimization step;
- the objective function is proportional to the total pumping power, and thus dependent on the product of the mass flow rate in each pumping branch and the pressure difference between the nodes between which it is located; for this reason, in this second step there are not only quadratic constraints, but the objective function itself is quadratic, making the optimization problem a MIQP (solved again using Gurobi).

$$\min_{\mathbf{t},\mathbf{G},\mathbf{P},\mathbf{G}_{\mathrm{aux}},\mathbf{B}} \sum_{i=1}^{N_{pumps}} G_i \Delta p_i \; s.t. \begin{cases} \mathbf{P} \geq p_{min} \\ \mathbf{P} \leq p_{max} \\ \mathbf{G} \leq \rho v_{max} \mathbf{S} \\ \mathrm{AG} + \beta \mathbf{G}^0_{\mathrm{ext}} = \mathbf{0} \\ \mathbf{A}^{\mathrm{T}} \mathbf{P} = (\mathbf{r} \odot \mathbf{G}_{\mathrm{aux}})\mathbf{G} - \mathbf{t} \\ \mathbf{P}(n_{BC}) = p_{BC} \\ \mathbf{G} + M\mathbf{B} \geq \mathbf{G}_{\mathrm{aux}} \\ -\mathbf{G} + M(\mathbf{1} - \mathbf{B}) \geq \mathbf{G}_{\mathrm{aux}} \\ \mathbf{G}_{\mathrm{aux}} \geq \mathbf{G} \\ \mathbf{G}_{\mathrm{aux}} \geq -\mathbf{G} \end{cases} \tag{9}$$

Overall, the two-step process (where the first step is a MIQCP problem and the second step is a MIQP problem) ensures not only that the mass flow is maximized to minimize the supply temperature (Step

1a), but also that the total pump power is the minimum possible for that specific configuration (Step 1b).

2.4. Step 2: identification of achievable supply temperature reduction

Once the maximum mass-flow rate allowed to circulate in the network is determined, it is needed to derive the corresponding minimum supply temperature achievable. This is achieved by cross-referencing the β obtained from the network analysis to the mass-flow rate increase required by the substation to operate with lower supply temperatures. The methodology developed in a previous study [35], including a substation model and a data analysis tool, can be effectively used to this purpose. This requires the knowledge of a sufficient amount of data collected at the DH substation in order to properly replicate the operation of the substation and to correctly estimate how the operation is modified when the supply temperature is lowered. In the mentioned work, and following the same methodology also in the present study, this is done by considering the substations as they are installed in their current state, without taking into account the possibility to make possible improvements on their design and/or operation.

The results are cross-referenced as illustrated in Fig. 4, as follows:

1. The mass-flow rate increase required by the substation as a function of the supply temperature reduction is defined: $\beta_{subst}(\Delta T_{supply})$. In this study, this is obtained using the methodology developed in Ref. [35].
2. The maximum mass-flow rate increase β allowed by the DH infrastructure and determined by the optimization methodology developed in this work is fixed.
3. The corresponding achievable ΔT for the infrastructure is determined.

This is repeated for each substation belonging to the examined network. In the end, the minimum supply temperature of the network is given by the maximum value of minimum supply temperature of the various substations connected to that network, leaving out thermal losses which should be properly estimated. The final value of minimum supply temperature identified represents the limitation to supply temperature reduction given by the existing DH infrastructure. It is worth highlighting that, for the whole system to operate in such conditions of reduced supply temperature, it is needed to take into account not only the minimum supply temperature achievable by the network (through the methodology developed in this study), but also the minimum supply temperature achievable by the substations (e.g. through the methodology developed in the referenced study [35]). Although the two conditions are interrelated, addressing them separately, as suggested by the proposed approach, allows to identify which is the part of the system that imposes the limit for the temperature reduction (if the network or the substations) and consequently suggests a direction for possible actions to improve the potential reduction in the system.

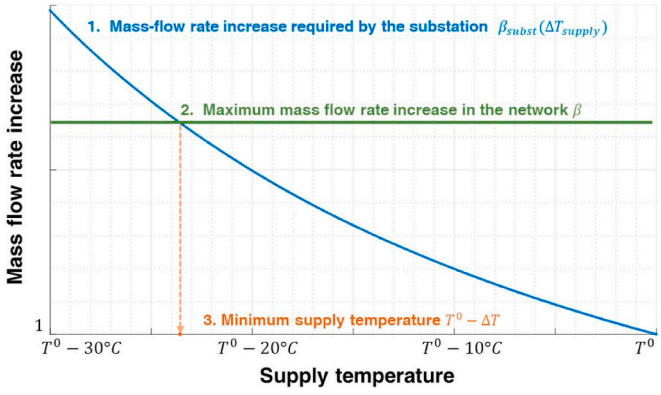

Fig. 4. Identification of the minimum supply temperature achievable by the network through a comparison of the maximum mass flow rate increase in the network and the mass flow rate increase required by the substations.

3. Case study

The proposed methodology is applied to a large-scale DH network installed in Italy and currently supplied by superheated hot water. The system satisfies the thermal request (mainly for space heating) of more than 7500 buildings, which have a total volume of about 71 million m^3.

The network can be thought of as consisting of two interconnected parts: the transportation network and the distribution networks. The transportation network is the core of the system and consists of pipes with larger diameters, connecting the thermal plants to the distribution networks in the different areas of the city. Then, the distribution networks, with smaller pipes, connect the transportation network to the buildings located in a certain area. The connection points between the transportation network and the various distribution networks are generally called thermal barycenters. In this work, the analysis is performed considering only the transportation network, since the distribution networks do not have specific fluid-dynamic problems, and thus the different buildings/substations connected to each distribution network can be grouped together for this type of analysis without loss of accuracy.

Six thermal production units are installed in the network. Three of them are Combined Heat and Power units, located in two areas in the North and South part of the city (one in Plant 2, and two in Plant 1) and producing up to 760 MW of heat. These plants supply the base load of the system. The production capacity is then completed by means of thermal energy storages (with a total capacity of 15000 m^3) and heat-only boilers. The nominal supply temperature in winter is about 120 °C, while in summer it is lowered to about 70 °C; while the temperature is kept approximately constant, the thermal load of the network is controlled by mass-flow rate regulation.

A typical winter steady condition is analyzed in this study. The reference mass-flow rate adopted for the simulation is 2210 kg/s, considering the current supply temperature equal to 120 °C. In these conditions, the thermal load is supplied by the two main plants, whose percentage contribution in terms of mass-flow rate is respectively 68 % from Plant 1 and 32 % from Plant 2. The objective of the study is to assess how much the total mass-flow rate can be increased and which would be the corresponding supply temperature reduction. Although the result is dependent on the location of the production plants and on their respective contribution to the supply of mass-flow rate, the choice of this configuration is coherent with the purpose of this work to analyze the existing infrastructure as is. Nevertheless, once this result is assessed, the methodology is also applied to other configurations in order to evaluate how much the final result can be improved by varying the percentage contribution of the different plants to the total supply; these configurations will be presented in the results section and are useful to assess possible improvements in the management of the system.

The minimization of supply temperature is achieved by acting on the different pumping stations located within the network infrastructure. In the analyzed DH network, different pumping stations are present in the transportation network, as reported in Fig. 5 where they are represented together with the topology of the network:

- the pumping groups located in the thermal plants (represented in green);
- the booster pumping stations, which are 9 in total; 8 of them are positioned on the supply network (represented in red), while 1 is located in the return network (represented in blue).

The management of the pressure rise of the pumps also allows to differently distribute the mass-flow rate among the various looping pipelines.

The methodology discussed in the previous section is applied to this

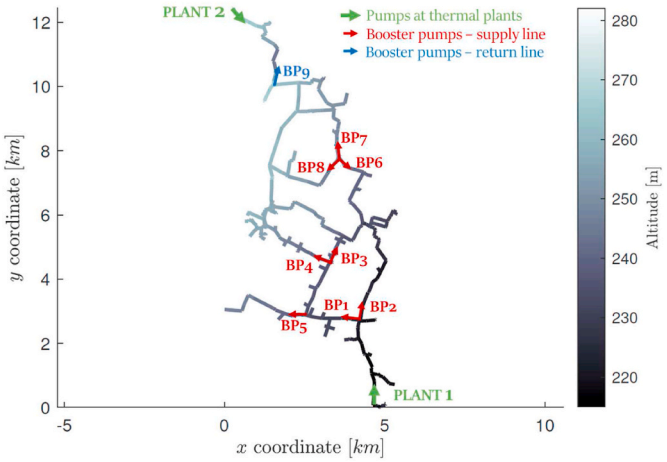

Fig. 5. Schematic of the case study: topology, location of pumping stations, altitude of the different areas of the city.

large-scale system to identify which is the maximum increase in the mass-flow rate achievable and, consequently, to estimate the corresponding potential for supply temperature reduction. The size of the analyzed problem proves the applicability of the method to problems of huge dimensions.

The analysis is performed adopting some precautionary assumptions. The maximum pressure allowed in this network is around 17 bar, which is adopted as upper boundary for the pressure optimization variables. The lower boundary is set to 2.5 bar as a precautionary measure to prevent evaporation (the current minimum pressure corresponding to the saturation pressure would be around 2 bar, considering a supply temperature of 120 °C; despite the analysis is done with the aim of decreasing the supply temperature, a safety conservative value of 2.5 bar is kept). Regarding the velocity constraint, it is imposed that its value within each pipeline cannot exceed 5 m/s. The minimum pressure drop across each distribution network is set to 2 bar (also in this case a cautionary value is used).

The altitudes of the different parts of the network are also reported in Fig. 5. The southern area of the city, where Plant 1 is located, has lower altitudes with respect to the other parts of the city. Thus, the mass-flow rate coming from Plant 1 needs to move uphill within the supply network, while it goes downhill in the return line. Considering Plant 2, the general trend is downhill in the supply network and uphill in the return network, but in this case there is also a valley in the first part of the supply line; a booster pump is inserted close to this valley within the return network to overcome the pressure losses and the geodetic head. All the other booster pumps are located within the supply network.

3.1. *Reference scenario: operation of the network at 120 °C*

In this section, a fluid-dynamic analysis is conducted on the reference scenario, involving the current operation of the system with supply temperature equal to 120 °C. In these circumstances, the mass flow rate required by the different distribution networks $\mathbf{G}^{\mathbf{0}}_{\mathrm{ext}}$ is known. To perform the analysis, it is supposed that the operation of the pumps is currently managed with the goal of minimizing the total pumping power. To this purpose, the optimizer developed in Step 1a Section 2.3 is used with a slightly different formulation since the multiplication factor is not needed in this case and $\mathbf{G}_{\mathrm{ext}} = \mathbf{G}^{\mathbf{0}}_{\mathrm{ext}}$.

The distribution of pressures and mass-flow rate obtained in this reference scenario is reported in Fig. 6. In the various figures, the width of the branches is proportional to the mass-flow rate, while the color reproduces the pressure magnitude according to the color bar reported nearby. Four graphs are reported in order to have a representation of the

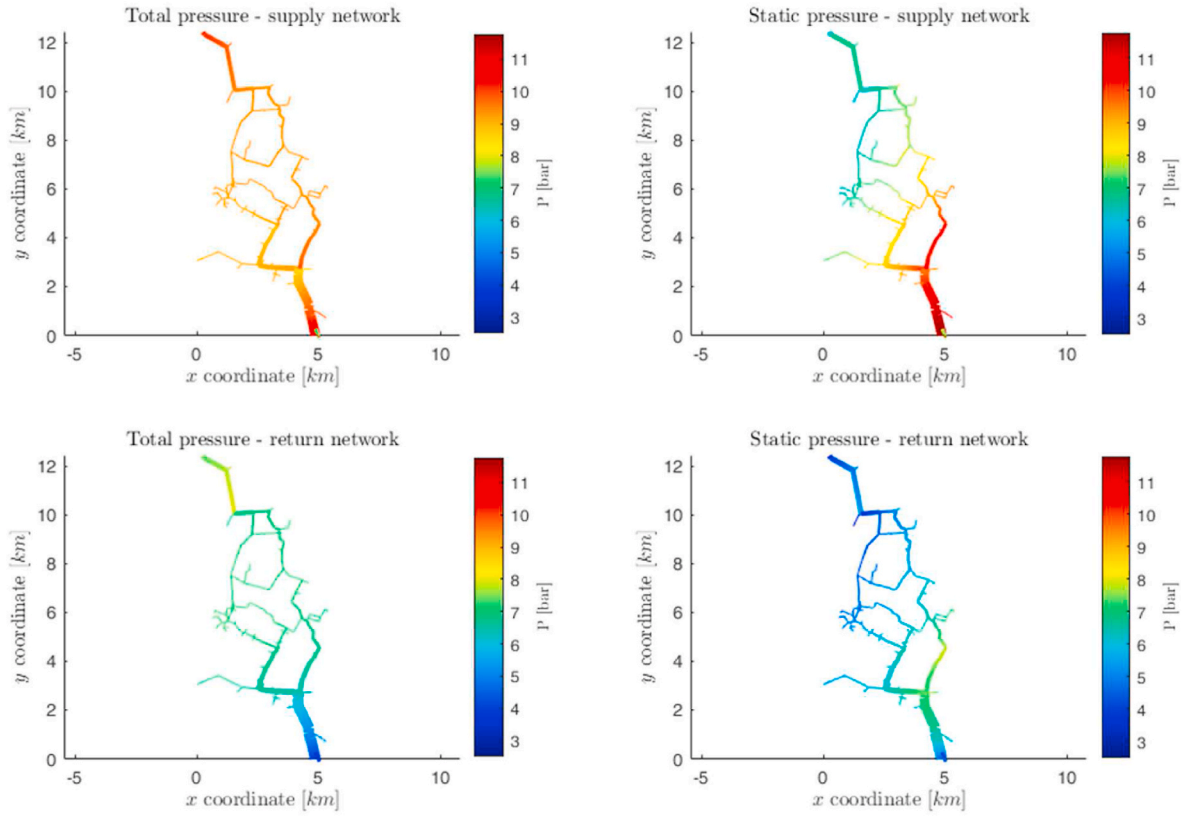

Fig. 6. Reference scenario (operation of the network at 120 °C): Distribution of static and total pressures along the supply and return lines of the network; the width of the branches is proportional to the distribution of mass flow rates.

fluid-dynamic situation on both the supply and return network and, in both of them, to be able to distinguish between total pressure and static pressure. The maximum value of the total pressure in the network in this configuration is 11.8 bar, and the maximum velocity observed is around 3 m/s and occurs in the main line from Plant 1. Globally, a pumping power of 1.6 MW is required for the operation of the pumps.

4. Results and discussion

This section reports and discusses the results of this study, starting with the results of the fluid-dynamic optimization (Section 4.1), then discussing the corresponding potential for temperature reduction (Section 4.2), and finally providing suggestions for possible ways to further reduce operating temperatures (Sections 4.4 and 4.5).

4.1. Step 1: improved operation at reduced temperature with increased mass flow rate

In this section, the two-step optimization approach discussed in Section 2.3 is applied to the transportation network of the case-study presented in Section 3. The calculation time is among the main strengths of the proposed approach, since the Gurobi optimizer takes only few minutes to converge with a final gap of 0.5 % for step 1a and 1 % for step 1b, using a computer with 128 GB of memory and an Intel Xeon CPU E5-2630 v3 @ 2.40 GHz processor.

From step 1a, it is possible to obtain the maximum mass flow rate increase that is achievable by the network with the specified constraints: the optimized value of β is 1.48, meaning that a +48 % mass-flow rate increase would be possible while satisfying all the constraints of the problem. The corresponding total mass-flow rate is 3279 kg/s. This increase is obtained by acting on the pressure rise of the different pumps located along the network. However, there could be multiple combinations of pressure rise of the different pumps allowing to work with the improved mass flow rate obtained from step 1a. For this reason, step 1b is adopted to identify the optimal operation of the pumps when working with the increased mass flow rate.

The distribution of pressures and mass-flow rate in the optimized configuration is reported in Fig. 7. The maximum value of the total pressure in the network corresponds to the upper bound that was imposed, equal to 17 bar. Because of the increase in the mass-flow rate, the energy required for pumping increases as well. The pressure rise and pumping power required by each pump in the improved configuration are compared to those of the reference scenario in Fig. 8. The total pumping power increases from 1.6 MW to 4.4 MW. Nevertheless, this 2.8 MW can be considered a good result since it is associated with a reduction in supply temperature (quantified in the next section) and with the corresponding exergy savings.

The velocity distribution in the network is reported in Fig. 9: the maximum velocity is observed again in the main line from Plant 1 it is equal to 4.5 m/s for both the supply and the return network. Looking at the results, it appears evident that this pipeline represents a fluid-dynamic bottleneck for possible mass-flow rate increases of the

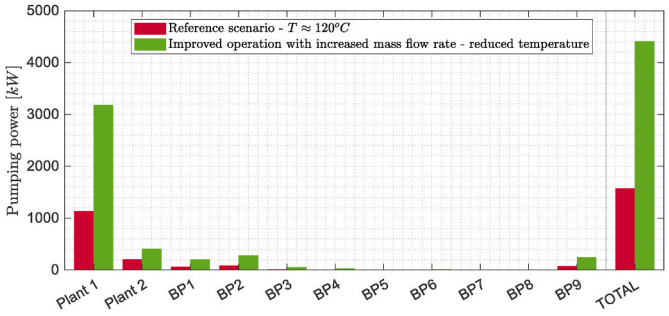

Fig. 8. Comparison of the pumping power required by the different pumps for the operation in the reference scenario (120 °C) and in the improved scenario (scenario with increased mass flow rate and reduced supply temperature).

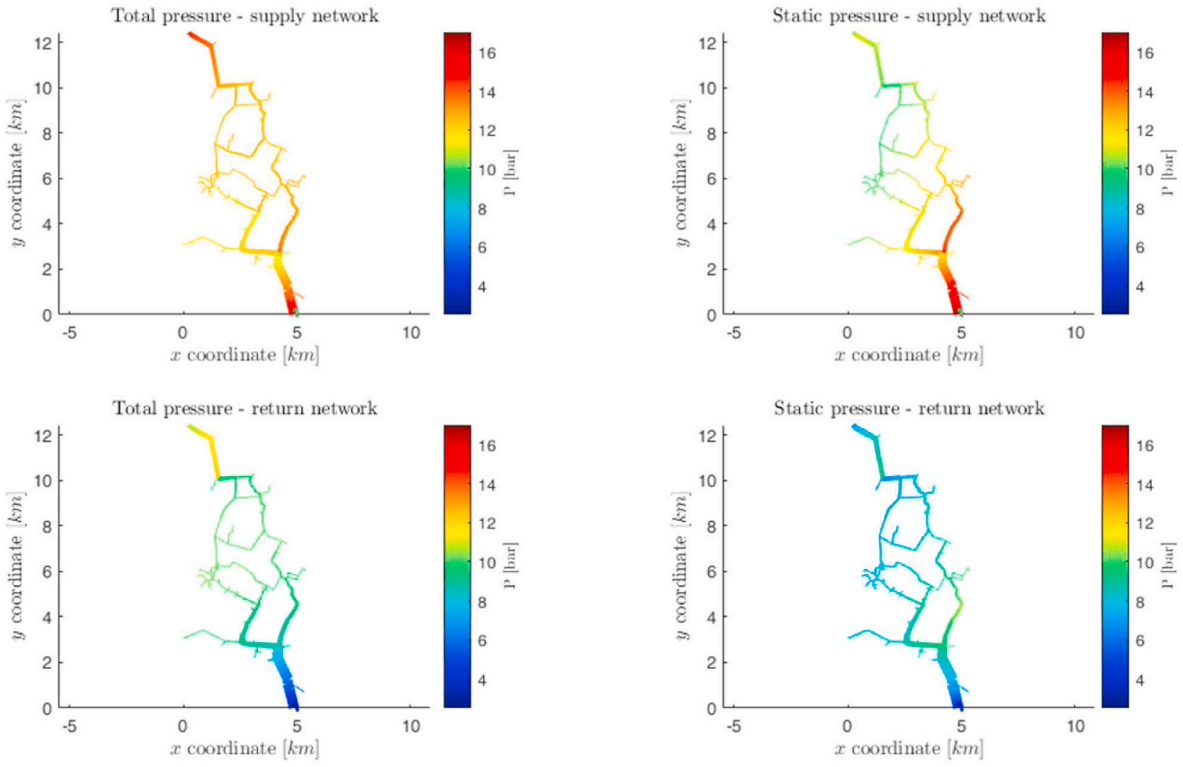

Fig. 7. Improved scenario (operation of the network at reduced supply temperature): Distribution of static and total pressures along the supply and return lines of the network; the width of the branches is proportional to the distribution of mass flow rates.

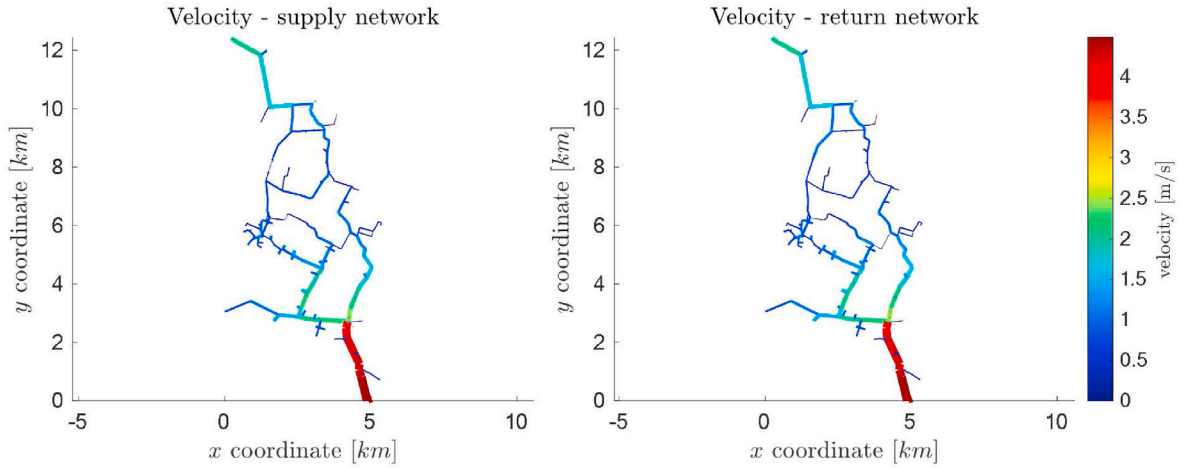

Fig. 9. Improved scenario (scenario with increased mass flow rate and reduced supply temperature): velocity distribution along the supply and return lines of the network.

network: in these ducts, the velocities are high and, consequently, the pressure losses that can be observed are significant.

4.2. Step 2: identification of the minimum supply temperature achievable with the improved operation

After having determined the maximum mass flow rate circulating in the network, it is possible to evaluate the corresponding reduction of flow temperature according to the methodology discussed in Section 2.4.

As explained in Section 3, the application discussed in this paper focuses on the analysis of the transportation network of a DH system installed in Italy. In order to identify the minimum supply temperature allowed by the transport infrastructure, it is necessary to know how the mass flow rate varies as a function of the supply temperature in the different distribution networks. This is obtained by performing a weighted average of the corresponding function of the different substations connected to the specific distribution network, being the substation function evaluated according to the methodology presented in Ref. [35]. Since data are available for only a part of the substations and distribution networks installed in the city, the missing data are assumed to have a similar behavior.

The mass-flow rate increase required by each distribution network as a function of the supply temperature is reported in Fig. 10. It is possible to see that with the limitation of the transportation network obtained at the previous step and equal to $\beta = 1.48$, the current potential of supply temperature reduction allowed by the infrastructure is between 18.5 °C and 20 °C, depending on the distribution network considered; considering a unique value of supply temperature for the whole network and taking into account that the current supply temperature is about 120 °C, it can be stated that a supply temperature of 102 °C is currently feasible for the DH network examined. This value does not represent the absolute minimum that can be achieved with the existing infrastructure, since it was obtained using conservative assumptions about the pressure and velocity limits; the result can rather be considered as an improvement, which is certainly feasible due to the careful choice of the assumptions. Nevertheless, it represents an excellent achievement since it allows to have exergy savings in the heat production of about 15 MW, which are far greater than the corresponding exergy increase associated with the operation of the pumps (which is around 3.5 MW considering a conversion efficiency of the pumps equal to 80 %).

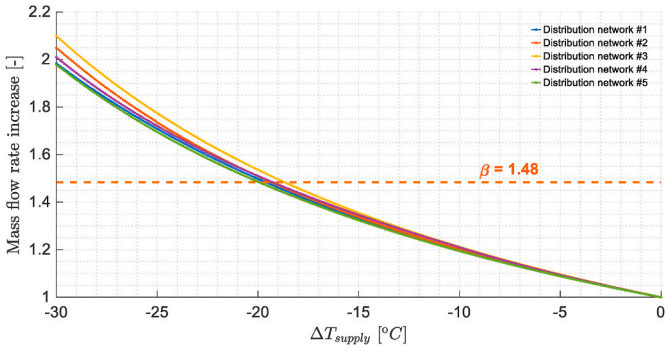

Fig. 10. Identification of the minimum supply temperature achievable in the case study through comparison of the maximum mass flow rate increase in the transportation network and the mass flow rate increase required by the different distribution networks.

It must be noted that the analysis presented here only guarantees that such a supply temperature value is sustainable by the network infrastructure, while it remains to be verified if the same value can also be feasible for the building/substation; in this specific case, results from the substations are available from the study presented in Ref. [35] and confirm the suitability of the obtained supply temperature also for the substation systems.

4.3. Analysis of different supply configurations and corresponding temperature reductions

The results of the study show the feasibility of currently supplying the network with a temperature of about 102 °C. This reduction can be achieved by considering the network as it is currently installed, without taking action on specific elements, without intervening in the current operating mode except for the supply temperature, and also by being conservative in the selection of the assumptions. Considering specific interventions in different parts of the system or different management strategies, further improvements can be achieved.

In this section, further analyses are carried out by changing the respective contributions of the main plants to the total supply. While the main pipeline of Plant 1 is congested, the main pipeline from Plant 2 is able to support further mass flow increases. For this reason, two additional configurations are tested in this analysis:

- A first further optimization is run by changing the respective contributions of the two plants from 68%-32 % to 60-40 %. In this case, a mass-flow rate increase of +66 % would be feasible, making it possible to further reduce the supply temperature to 96–98 °C. However, the possibility of modifying the load share of the plant

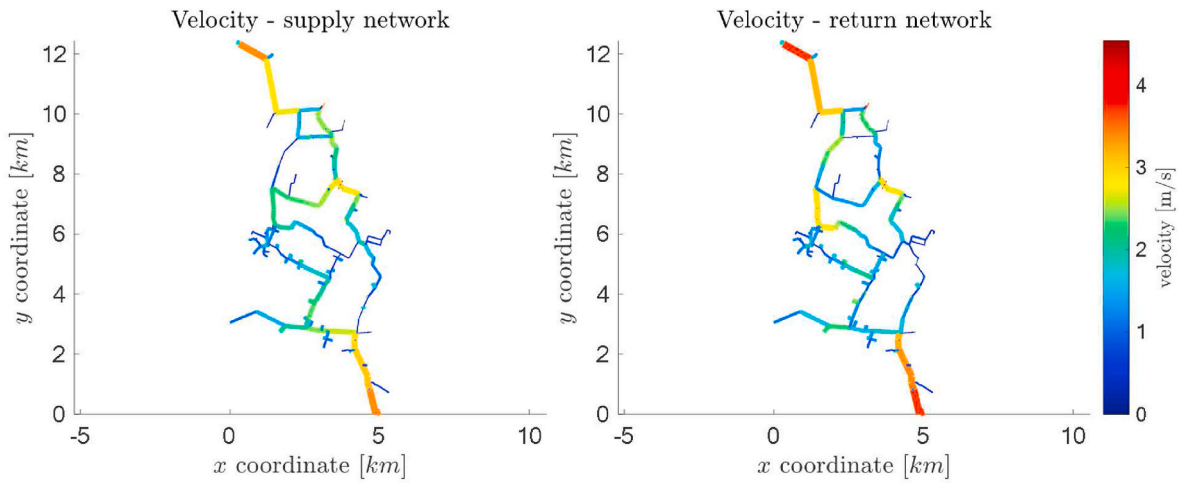

Fig. 11. Improved scenario (operation of the network at reduced supply temperature) and modified mass flow rate supply: velocity distribution along the supply and return lines of the network.

must be verified since it is associated to the size of the generation units installed.

- A final configuration is also analyzed by considering mass-flow rate injections from additional parts of the network, as is the case for example when using thermal energy storages located in the transport network. The configuration analyzed in this case involves the 70 % of mass-flow rate being provided by Plant 1 and Plant 2, while the remaining 30 % is supplied by thermal storages located in other parts of the network and being charged during the night. In this case, mass flow rates are more homogeneously distributed and the velocities along the network appear more uniform, as evident from Fig. 11. This configuration brings to a maximum mass-flow rate increase of +140 % ($\beta = 2.4$), which is compatible with a supply temperature even lower than 90 °C. Also in this case, the configuration is feasible considering the fluid dynamic behavior of the network, but it must be verified in terms of thermal power supply of the various plants.

Other possible configurations could be analyzed adopting the same methodology. This becomes very useful when considering the possibility of integrating additional renewable energy sources in the network that could be located in different locations than the ones of the main plants. Moreover, the results suggest promising opportunities when shifting to distributed generation.

4.4. Suggested strategies for further reducing operating temperatures

Other possible solutions could be considered to achieve further reductions in the operating temperatures of the system. Some useful recommendations are the following:

- One possible strategy to further reduce the supply temperature of the network is to act on the parts of the network that cause bottlenecks in reducing the supply temperature. From the fluid-dynamic results obtained in this study, it is possible to see that the main issues occur in the main pipeline connected to Plant 1, where the flow velocity and the pressure drop are high. Since the area presenting the main bottlenecks is clearly defined, it could be useful to analyze the possibilities of replacing these pipelines with larger ones, which would reduce the velocity and pressure drops, thus allowing the possibility of further increasing the mass flow and reducing the supply temperature.
- Finally, it would be advisable to analyze the possibilities of varying the supply temperature according to the outdoor temperature conditions. In this study, a single value of supply temperature was considered for the whole heating season. For this reason, the minimum supply temperature achievable is the one corresponding to the coldest days of the year; during milder days, a lower value of supply temperature would be possible for the district heating network, since the demands of the buildings are typically lower. A dynamic temperature approach can be analyzed to exploit the possibility of varying the supply temperature of the network during the year, making it possible to further reduce the operating temperature when the outdoor conditions allow it.

5. Conclusions

This paper presents a new approach to identify the potential for supply temperature reduction of existing district heating networks, focusing on the transportation infrastructure and on the hydraulics of the whole system. This potential is related to the mass flow rate that can be circulated in the network: the lower the supply temperature, the higher is the mass flow rate needed by the substations to provide to the building the required thermal demand. For this reason, a tailored methodology is developed to 1) maximize the mass flow rate that can be processed by an existing infrastructure (keeping as lower as possible the pumping power increase), and 2) identify the minimum supply temperature corresponding to the maximum mass flow increase according to the operation of the thermal substations. To reach these targets, it is supposed to act on elements that are already installed in the network: the pressure rise of the different pumps are the optimization variables of the problem and can be adjusted to differently distribute mass flow rates in the different looping branches in order to improve the operation of the network and minimize the supply temperature.

The optimization approach includes a fluid dynamic model of the network, which allows the analysis of all possible bottlenecks that may occur within the network and ensures compliance with specific velocity and pressure constraints. It also includes an optimization step focused on the minimization of the total pumping power which allows to avoid an excessive high increase of the pumping costs associated with the higher mass flow rates required by the low temperature operation. The different optimization steps are formulated as MIQCP and MIQP problems and can be applied to different networks from small to large scale.

The methodology is applied to a large-scale case study: a network of huge dimensions located in Italy is analyzed. Despite the complexity of the case study, the optimization approach provides fast and promising results. The mass flow rate increase obtained through the optimization approach is expected to reduce the supply temperature of the network from 120 °C to about 102 °C considering the current supply configuration from the two main plants. Further reductions up to 90 °C can be obtained when considering a more distributed heat generation, in this

case by using heat storages located along the network to decouple production and consumption. This is a crucial result, especially considering that no structural changes are taken into account and that even better results can be obtained by acting on specific elements of the network (for example, replacing the most critical pipelines) or by changing the supply management. Moreover, it proves the applicability of the proposed methodology to existing networks of large scale and with complex topologies.

Overall, the methodology presented in this work represents a novel and powerful tool for optimizing mass flow rates in existing district heating networks to effectively achieve temperature reductions without the need for structural interventions, thus making a significant contribution to the transition of existing infrastructures to next-generation systems.

CRediT authorship contribution statement

Martina Capone: Writing – original draft, Software, Methodology, Investigation, Data curation, Conceptualization. **Elisa Guelpa:** Writing – review & editing, Supervision, Methodology, Funding acquisition, Conceptualization. **Vittorio Verda:** Supervision, Resources, Methodology, Conceptualization.

Declaration of competing interest

The authors declare that they have no known competing financial interests or personal relationships that could have appeared to influence the work reported in this paper.

Data availability

The authors do not have permission to share data.

Acknowledgements

The preliminary results of this analysis have been made possible thanks to funding from IEA DHC (The International Energy Agency Technology Collaboration Programme on District Heating and Cooling), as a part of the project “Leave 2nd generation behind: cost effective solutions for small-to-large scale DH networks”, financed by IEA DHC within Annex XIII. Project partners are Politecnico di Torino, University of Birmingham and CEA - Commissariat à l’énergie atomique et aux énergies alternatives.

The authors would like to express their sincere gratitude to the managing company of the analyzed district heating system for sharing the topological information of the network.

APPENDIX

The complete formulation of the optimization problem described in Equation (5) is reported in Equation (A.1).

$$\max_{\beta,\mathbf{t}_{supply},\mathbf{G}_{supply},\mathbf{P}_{supply},\mathbf{t}_{return},\mathbf{G}_{return},\mathbf{P}_{return}} \beta$$

$$s.t. \begin{cases} \beta \geq 1 \\ \mathbf{P}_{supply} \geq p_{min} \\ \mathbf{P}_{supply} \leq p_{max} \\ \mathbf{G}_{supply} \leq \rho v_{max} \mathbf{S}_{supply} \\ \mathbf{A}_{supply}\mathbf{G}_{supply} + \beta \mathbf{G}^{0}_{ext,supply} = \mathbf{0} \\ \mathbf{A}^{\mathbf{T}}\mathbf{P}_{supply} + \rho g \mathbf{A}^{\mathbf{T}}\mathbf{z}_{supply} = \mathbf{R}_{supply}(\mathbf{G}_{supply})\mathbf{G}_{supply} - \mathbf{t}_{supply} \\ \mathbf{P}_{supply}(n_{BC}) = p_{BC} \\ \mathbf{P}_{return} \geq p_{min} \\ \mathbf{P}_{return} \leq p_{max} \\ \mathbf{G}_{return} \leq \rho v_{max} \mathbf{S}_{return} \\ \mathbf{A}_{return}\mathbf{G}_{return} + \beta \mathbf{G}^{0}_{ext,return} = \mathbf{0} \\ \mathbf{A}^{\mathbf{T}}\mathbf{P}_{return} + \rho g \mathbf{A}^{\mathbf{T}}\mathbf{z}_{return} = \mathbf{R}_{return}(\mathbf{G}_{return})\mathbf{G}_{return} - \mathbf{t}_{return} \\ \mathbf{P}_{supply}(n_{ext}) - \mathbf{P}_{return}(n_{ext}) \geq \Delta p_{min,n_{ext}} \end{cases} \quad (A.1)$$

References

[1] Rivas S, Urraca R, Bertoldi P, Thiel C. Towards the EU Green Deal: local key factors to achieve ambitious 2030 climate targets. J Clean Prod Oct. 2021;320:128878. https://doi.org/10.1016/J.JCLEPRO.2021.128878.

[2] International Energy Agency. Renewable heat. 2021. https://doi.org/10.1016/s1471-0846(05)00330-6.

[3] Frederiksen S, Werner S. District heating and cooling. Studentlitteratur AB; 2013.

[4] Lund H, et al. 4th Generation District Heating (4GDH). Integrating smart thermal grids into future sustainable energy systems. Energy 2014;68:1–11. https://doi.org/10.1016/j.energy.2014.02.089.

[5] Lund H, et al. The status of 4th generation district heating: research and results. Energy 2018;164:147–59. https://doi.org/10.1016/j.energy.2018.08.206.

[6] Lund H, et al. Perspectives on fourth and fifth generation district heating. Energy Jul. 2021;227:120520. https://doi.org/10.1016/J.ENERGY.2021.120520.

[7] Lygnerud K, Popovic T, Schultze S, Støchkel HK. District heating in the future - thoughts on the business model. Energy Sep. 2023;278:127714. https://doi.org/10.1016/J.ENERGY.2023.127714.

[8] Merlet Y, Baviere R, Vasset N. Optimal retrofit of district heating network to lower temperature levels. Energy Nov. 2023;282:128386. https://doi.org/10.1016/J.ENERGY.2023.128386.
[9] Yuan M, et al. Renewable energy and waste heat recovery in district heating systems in China: a systematic review. Energy May 2024;294:130788. https://doi.org/10.1016/J.ENERGY.2024.130788.
[10] Qin Q, Gosselin L. Multiobjective optimization and analysis of low-temperature district heating systems coupled with distributed heat pumps. Appl Therm Eng Jul. 2023;230:120818. https://doi.org/10.1016/J.APPLTHERMALENG.2023.120818.
[11] Stock J, Arjuna F, Xhonneux A, Müller D. Modelling of waste heat integration into an existing district heating network operating at different supply temperatures. Smart Energy May 2023;10:100104. https://doi.org/10.1016/J.SEGY.2023.100104.
[12] Rämä M, Pursiheimo E, Sundell D, Abdurafikov R. Dynamically distributed district heating for an existing system. Renew Sustain Energy Rev Jan. 2024;189:113947. https://doi.org/10.1016/J.RSER.2023.113947.
[13] Guelpa E, Capone M, Sciacovelli A, Vasset N, Baviere R, Verda V. Reduction of supply temperature in existing district heating: a review of strategies and implementations. Energy 2023;262:125363. https://doi.org/10.1016/j.energy.2022.125363.
[14] Guelpa E, et al. Leave 2nd generation behind: cost effective solutions for small-to-large scale DH networks - IEA DHC Annex XIII report. 2023.
[15] Chicherin S, Zhuikov A, Junussova L. 4th generation district heating (4GDH) in developing countries: low-temperature networks, prosumers and demand-side measures. Energy Build Sep. 2023;295:113298. https://doi.org/10.1016/J.ENBUILD.2023.113298.
[16] Volkova A, Koduvere H, Pieper H. Large-scale heat pumps for district heating systems in the Baltics: potential and impact. Renew Sustain Energy Rev Oct. 2022;167:112749. https://doi.org/10.1016/J.RSER.2022.112749.
[17] Schlosser F, Jesper M, Vogelsang J, Walmsley TG, Arpagaus C, Hesselbach J. Large-scale heat pumps: applications, performance, economic feasibility and industrial integration. Renew Sustain Energy Rev Nov. 2020;133:110219. https://doi.org/10.1016/J.RSER.2020.110219.
[18] Østergaard DS, Svendsen S. Experience from a practical test of low-temperature district heating for space heating in five Danish single-family houses from the 1930s. Energy 2018;159:569–78. https://doi.org/10.1016/j.energy.2018.06.142.
[19] Dalla Rosa A, et al. Toward 4 th generation district heating. Experience and potential of low-temperature district heating - IEA DHC Annex X report. 2014 [Online]. Available: http://www.iea-dhc.org/the-research/annexes/2011-2014-annex-x/annex-x-project-03.html.
[20] Averfalk H, et al. Low-temperature district heating implementation guidebook - final report of IEA DHC Annex TS2. Technology Collaboration Programme by IEA; 2021.
[21] Li H, Svendsen S. Energy and exergy analysis of low temperature district heating network. Energy 2012;45(1):237–46. https://doi.org/10.1016/j.energy.2012.03.056.
[22] Helge Averfalk LQ, Werner Sven, Felsmann Clemens, Rühling Karin, Wiltshire Robin, Svendsen Svend, Li Hongwei, Faessler Jerome, Mermoud Floriane. Transformation roadmap from high to low temperature district heating systems - final report of IEA DHC Annex XI. Annex XI Final Rep. -Transformation Roadmap from High to Low Temp. Dist. Heat. Syst. 2017.
[23] Rämä M, Sipilä K. Transition to low temperature distribution in existing systems. Energy Proc 2017;116:58–68.
[24] Dino GE, Catrini P, Buscemi A, Piacentino A, Palomba V, Frazzica A. Modeling of a bidirectional substation in a district heating network: validation, dynamic analysis, and application to a solar prosumer. Energy Dec. 2023;284:128621. https://doi.org/10.1016/J.ENERGY.2023.128621.
[25] Cenian A, Dzierzgowski M, Pietrzykowski B. On the road to low temperature district heating. J. Phys. Conf. Ser. 2019;1398(1). https://doi.org/10.1088/1742-6596/1398/1/012002.
[26] Mikielewicz J, Ochrymiuk T, Cenian A. Comparison of traditional with low temperature district heating systems based on organic Rankine cycle. Energy Apr. 2022;245:123280. https://doi.org/10.1016/J.ENERGY.2022.123280.
[27] Schmidt D, et al. Successful implementation of low temperature district heating case studies. Energy Rep 2021;7(September):483–90. https://doi.org/10.1016/j.egyr.2021.08.079.
[28] Lumbreras M, Garay R. Energy & economic assessment of façade-integrated solar thermal systems combined with ultra-low temperature district-heating. Renew Energy Oct. 2020;159:1000–14. https://doi.org/10.1016/J.RENENE.2020.06.019.
[29] Werner S. Network configurations for implemented low-temperature district heating. Energy 2022;254:124091. https://doi.org/10.1016/J.ENERGY.2022.124091.
[30] Volkova A, et al. Cascade sub-low temperature district heating networks in existing district heating systems. Smart Energy Feb. 2022;5:100064. https://doi.org/10.1016/J.SEGY.2022.100064.
[31] Puschnigg S, Jauschnik G, Moser S, Volkova A, Linhart M. A review of low-temperature sub-networks in existing district heating networks: examples, conditions, replicability. Energy Rep Oct. 2021;7:18–26. https://doi.org/10.1016/J.EGYR.2021.09.044.
[32] Volkova A, et al. Energy cascade connection of a low-temperature district heating network to the return line of a high-temperature district heating network. Energy 2020;198. https://doi.org/10.1016/j.energy.2020.117304.
[33] Nagy Z, Rossi D, Hersberger C, Irigoyen SD, Miller C, Schlueter A. Balancing envelope and heating system parameters for zero emissions retrofit using building sensor data. Appl Energy 2014;131:56–66. https://doi.org/10.1016/J.APENERGY.2014.06.024.
[34] Hesaraki A, Bourdakis E, Ploskić A, Holmberg S. Experimental study of energy performance in low-temperature hydronic heating systems. Energy Build 2015;109:108–14. https://doi.org/10.1016/J.ENBUILD.2015.09.064.
[35] Capone M, Guelpa E, Verda V. Potential for supply temperature reduction of existing district heating substations. Energy Dec. 2023;285:128597. https://doi.org/10.1016/J.ENERGY.2023.128597.
[36] Brange L, Lauenburg P, Sernhed K, Thern M. Bottlenecks in district heating networks and how to eliminate them – a simulation and cost study. Energy Oct. 2017;137:607–16. https://doi.org/10.1016/J.ENERGY.2017.04.097.
[37] Guelpa E, Sciacovelli A, Verda V. Thermo-fluid dynamic model of large district heating networks for the analysis of primary energy savings. Energy 2019;184:34–44. https://doi.org/10.1016/j.energy.2017.07.177.
[38] Capone M, Guelpa E, Verda V. Accounting for pipeline thermal capacity in district heating simulations. Energy Mar. 2021;219:119663. https://doi.org/10.1016/J.ENERGY.2020.119663.
[39] Harary F. Graph theory. New Delhi: Narosa Publishing; .
[40] V Patankar S, Spalding DB. A calculation procedure for heat, mass and momentum transfer in three-dimensional parabolic flows. Int J Heat Mass Tran 1972;15:1787–806.
[41] Guelpa E, Toro C, Sciacovelli A, Melli R, Sciubba E, Verda V. Optimal operation of large district heating networks through fast fluid-dynamic simulation. Energy 2016;102. https://doi.org/10.1016/j.energy.2016.02.058.
[42] Bezanson J, Edelman A, Karpinski S, Shah VB. Julia: a fresh approach to numerical computing. SIAM Rev 2017;59(1):65–98.
[43] Gurobi Optimization. Gurobi optimizer reference manual. 2022. https://www.gurobi.com.